

Continuous electro-oxidation of lignin to vanillic and syringic acid at near 100 mA·cm⁻²

Salvador Montilla-Verdú^[a], Xavier Marset^[a], Elio Rico^[a], Maxime Contreras^[a], Antonio Rodes^[a], Néstor Guijarro^[a] *

^[a] Institute of Electrochemistry, Universidad de Alicante, Apdo. 99, 03080 Alicante, Spain.

Abstract

The use of lignin as a renewable feedstock for valuable chemicals has gained significant momentum due to the ongoing depletion of fossil fuel reserves and the environmental harm caused by their overuse. However, extracting useful products from this recalcitrant biopolymer requires a highly selective fragmentation process. This article demonstrates that such a process can be effectively achieved through an electrochemical approach. While Ni- and Co-based catalysts have been previously employed for lignin electrooxidation, the optimal composition of mixed metal oxyhydroxides—crucial for achieving higher yields and faradaic efficiencies—has not been thoroughly investigated until now. This optimization was made possible by a comprehensive study beginning with lignin model compounds, which elucidated the reaction mechanism and facilitated the subsequent scaling of the reaction using organosolv pine lignin. Remarkably, this approach yielded up to 6.0 wt% vanillic acid. These unprecedented results were achieved through the meticulous design of an electrochemical flow cell, ensuring that the electrochemical production of lignin monomers is not only cost-effective and selective but also easily scalable.

Introduction

Chemical industry has been supplied with petrol-derived feedstocks, but the depletion of fossil reserves and the instability derived from market fluctuation highlighted the urgent need to seek renewable resources as carbon source. In this sense, lignocellulosic biomass, such as forestry and agriculture residues, which is the most abundant renewable resource of organic carbon^{1,2} has been proposed as an alternative. This raw material comprises carbohydrates (cellulose and hemicellulose) and a polymer-rich in aromatics (lignin). Over the years, cellulose has been widely valorized in cellulose pulping processes for paper manufacturing. However, lignin waste is discarded in this process and used as a low-grade fuel to obtain heat and energy or low-value resins and lubricants^{2–5}. Nevertheless, given its structure, rich in aromatic units derived from p-hydroxyphenyl (H), guaiacyl (G), and syringyl (S) motifs, this biopolymer could be the replacement of fossil reserves for the obtention of high-value aromatics compounds useful as chemical feedstock in several industrial sectors.^{5–8} However, lignin's amorphous tridimensional structure is composed subunits crosslinked by C–C and C–O–C bonds^{9–12}, being β–O–4 ether bonds the most abundant (45–60% of the total linkages)^{11,12} this recalcitrant structure supposes a great challenge for achieving a selective and cost-efficient fragmentation without deteriorating useful structures. For this reason, the main aim of this research is the selective C_α–C_β oxidative cleavage of this structure to produce, mainly, vanillic and syringic acids.

In recent years, different technologies have been developed for lignin depolymerization, including i) biological, ii) thermal, and iii) chemical catalytic methods^{1–4}. However, these methods show numerous disadvantages that are difficult to solve. For example, thermal processes such as pyrolysis, hydrothermal liquefaction, or microwave-assisted depolymerization require high temperatures and/or pressures causing the destruction of valuable products by secondary reactions and undesirable re-polymerization^{2,4,13,14}, as well as being energetically inefficient. Chemical catalytic methods (Base/Acid-Catalysis, oxidation, or Ionic Liquid-Assisted depolymerization) typically require lower temperature and have better control over the reaction, but requirement of using high pressures and the use of expensive catalysts and reagents greatly

increase the economic cost, which adds to the environmental hazards derived from the use of unsafe chemical reagents.^{2,4,12,15} Finally, most of these problems could be solved using biological depolymerization, which presents cost-effectiveness and specificity, but these methods are still inefficient for large applications, having low reaction rates and yields^{4,16,17}. Thus, a green technology able to offer high yields and selectivity without compromising the safety and economical cost is required, and in this sense is where electrochemistry comes into play. Electrochemical technologies are most effective for controlling the reactions because it is possible to work under mild conditions (room temperatures and pressures) and can be coupled to other reactions, for example, hydrogen evolution reaction (HER), increasing the global value of the process and minimizing waste generation. Thus, we envisioned the use of a solid-state catalyst as an electrode to directly oxidize lignin on the electrode surface^{1,18}. This strategy allows to easily recover and reuse the catalyst without contaminating the reaction mixture with metals, which is especially relevant if the obtained products are intended to be used as raw materials in the alimentary or pharmaceutical industries.

In literature, most research reported on this kind of catalyst for lignin electro-oxidation is based on the use of IrO₂^{10,18–20}, Pb/PbO₂^{18,21–24}, Ni^{18,25–27} and Ni-Co^{9,18,28,29} alloys as anode showing promising results. For instance, Smith *et al.*²⁶ employed cylindrical nickel electrodes as anodes in a flow reactor operating at 145°C, 5 bar, 8 A (1.9 mA cm⁻²) for 3.5 h. and a solution of NaOH 3 M as reaction media and achieving the electro-oxidative conversion at laboratory scale of a lignosulfonate (61 gL⁻¹) into vanillin. The yields obtained from this monomer were similar to those obtained industrially using chemical oxidants (about 5.7% w/w). Other studies using Nickel include those reported by Zirbes *et al.*²⁷ achieved yields of vanillin about 4.2 w/w using kraft lignin (6 gL⁻¹), nickel foam as anode, an undivided stainless-steel cell and operating at 160°C, 10 mA cm⁻², 6.5 h. Moreover, Breiner *et al.*³⁰ used a simple autoclave electrolysis cell and a planar nickel anode to carry out high-temperature electrolysis of straw organosolv lignin (9 gL⁻¹) operating to 180°C, 15 mA cm⁻², obtaining 2.5% w/w vanillin and 1.8% w/w syringaldehyde as monomer yields. However, these high temperatures and pressures make scaling up to an industrially useful range a challenging task and economically noncompetitive. Therefore, performing those reactions under ambient conditions (temperatures and pressures) is much more desirable, but traditionally, the yields of vanillin and vanillic acid obtained by such methods are very low^{31,32} (Table S1) reaching an apparent limit due to an equilibrium between the formation of monomeric products, its concomitant oxidative destruction to CO₂, and further condensation of lignins. In this sense, Ghahremani *et al.*³¹ reported the lignin electrochemical oxidation in the presence of nickel (Ni), cobalt (Co), and Ni-Co bimetallic electrocatalysts at room temperature, concluding that the rate of electrochemical oxidation of lignin is higher with Ni-Co bimetallic electrocatalysts with higher Co contents. However, the obtained yields remained low and the optimal Co content was not deeply surveyed, offering room for much improvement. In this line, this study aims to optimize the metallic composition of an electrocatalyst to obtain monomeric yields under ambient temperature and pressure conditions.

In addition, there are other problems to sort out: i) the competence with the oxygen evolution reaction (OER) that decreases the faradaic efficiency of the reaction, ii) mechanistic studies to be able to understand and control the reactions and iii) the electrocatalyst composition of active metals. Consequently, in the present research, a series of Fe_{1-x-y}Co_yNi_xOOH samples were synthesized using an organometallic decomposition method and tested as electrocatalysts for benzyl alcohol (BA) and 1-Phenylethanol (PEA) oxidation to the corresponding carbonylic compounds to optimize the metallic composition required for maximizing the catalytic activity while minimizing OER. Having determined the optimal electrocatalyst (Ni_{0.75}Co_{0.25}OOH) a study of electrochemical oxidative cleavage of a series of lignin dimeric models was performed, as well as with a polymeric lignin model which shed light on the reaction mechanism. Finally, the depolymerization of organosolv lignin was achieved.

Results and Discussion

A series of 27 amorphous mixed-metal oxide films formulated as $\text{Fe}_{1-y-x}\text{Co}_y\text{Ni}_x(\text{OH})_2$, where y and z depend on the proportion of the three metals, were prepared by a process of organometallic decomposition as described in the supporting, using Fluoride Tin Oxide Glass (FTO) as conductor substrate³³. These electrodes were tested by cyclic voltammetry (CV) to optimize the metal proportion of Fe-Ni-Co. $\text{Ni}_{0.75}\text{Co}_{0.25}\text{OOH}$ electrocatalyst was initially evaluated for electrochemical oxidation of Benzyl alcohol (BA), 1-phenylethanol (PEA), and lignin dimer 2 (entry 2, Table 1) (indicated in Table 1), typical lignin models compound with C(OH)-C structure. The goal was to use BA as a simple lignin model to study the oxidation of the OH in C_α , PEA to study the cleavage of the $\text{C}_\alpha\text{-C}_\beta$ bond, and dimer to assess how effectively the $\beta\text{-O-4}$ linkage is cleaved. As shown in Figure 1a, the CV curve of $\text{Ni}_{0.75}\text{Co}_{0.25}(\text{OH})_2$ shows an oxidation band between 1.25-1.40 vs RHE that corresponds to the oxidation of $\text{Ni}_{0.75}\text{Co}_{0.25}(\text{OH})_2$ to $\text{Ni}_{0.75}\text{Co}_{0.25}\text{OOH}$, the active phase³³⁻³⁶. Moreover, the Oxygen Evolution Reaction (OER) appears in 1.0 M KOH electrolyte with an onset overpotential of 290 mV. To our delight, introducing lignin models into the electrolyte led to a significant reduction of onset potential, indicating the lower energy barrier of these oxidations than that of OER³⁷. The onset potential approximately coincides with the electrochemical activation potential, which is why it appears to be the limiting process for this type of electro-oxidation reaction. Next, the other 26 mixed-metal electrodes were tested by CV to evaluate their performance of electrochemical oxidation of BA, PEA, dimer 2, and OER. Figure 1b shows a ternary diagram that presents the potential required to achieve 5 mA cm^{-2} current to OER. As can be seen, electrocatalysts with a similar proportion of Ni-Fe-Co present the highest activity to OER performance³⁸. Figures 1 c, d, and e display the potential required to achieve 5 mA cm^{-2} current to lignin model oxidation and it is compared with OER performance to analyze the reduction of onset potential. As shown, electrocatalysts with a high OER performance exhibit relatively low lignin model oxidation activity. Thus, the best electrocatalysts turned out to be $\text{Co}_y\text{Ni}_x\text{OOH}$ ($y=0\text{-}0.75$, $x=1\text{-}0.25$) which shows that OER response is relatively low. These results are positive because the proportion of metals can be modulated to favor catalytic activity towards the desired products and minimize the competition reaction (OER). In addition, the four best electrocatalysts were synthesized upon carbon felt (CF) and tested in reaction (BA and PEA oxidation) by chronoamperometry at 1.5V vs RHE for 4 hours (Figures S5-S9). $\text{Ni}_{0.75}\text{Co}_{0.25}\text{OOH}$ manifesting the best electrochemical performance and the highest product yields and faradaic efficiencies, was assigned as the optimal electrocatalyst. For this reason, the rest of the experiments were carried out only with this electrocatalyst.

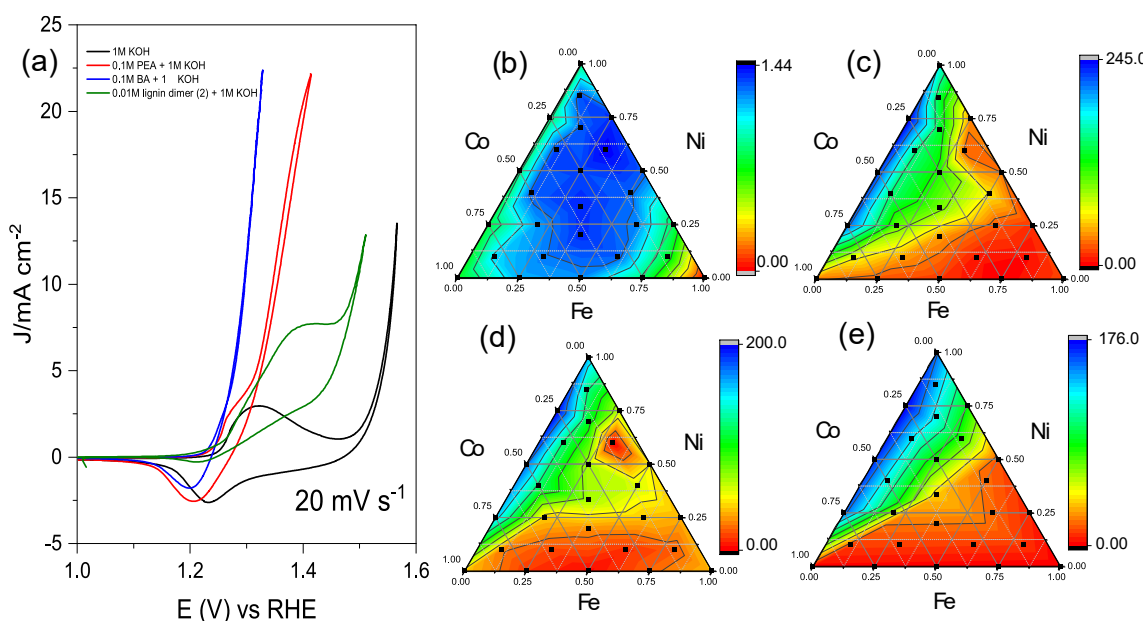


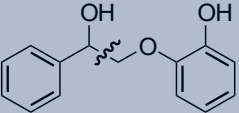
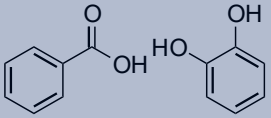
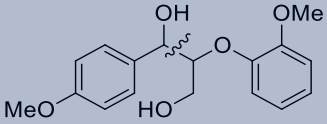
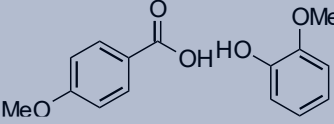
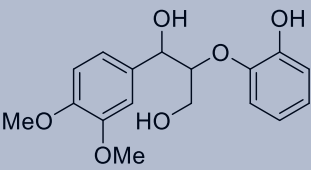
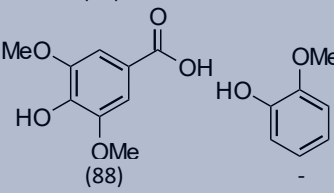
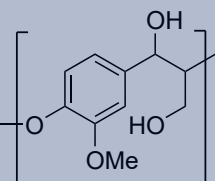
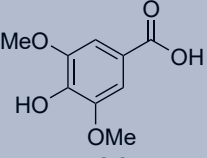
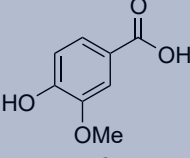
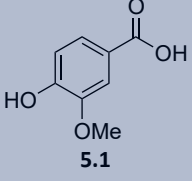
Figure 1. Optimization of the composition of the electrocatalyst (a) cyclic voltammetry (20mV s⁻¹) with Ni_{0.75}Co_{0.25}OOH as electrocatalyst to BA, PEA, dimer 2 and water oxidation (IR corrected), (b,c,d,e) Fe–Ni–Co ternary composition plot for (b) OER (c) BA, (d) PEA and (e) dimer 2.

After optimization work, different lignin dimers with a β -O-4 linkage were tested to study the fragmentation efficiency of the major bond present in the lignin structure (Table 1, entries 1,2,3). All dimers exhibit high conversion and yield towards the aromatic monomer with carboxylic acid as major product^{39,40}, which is the high-value monomeric species that we were expecting to obtain. However, the other fragment that forms the dimer (catechol or guaiacol) could not be detected by ¹H-NMR. To study this setback, an experiment was carried out with 0.01M of guaiacol and/or catechol under the same reaction conditions. The results showed the instability of guaiacol in oxidative conditions, since the ¹H-NMR signals of these compounds disappeared and others identical to those obtained in the oxidation reactions of the dimers appeared (Figure S10). For this reason, we can conclude that these compounds decompose in the reaction medium, evolving into other by-products. In the literature^{41,42}, different authors report that electrooxidation of guaiacol produces different compounds derivatives of maleic acid and oxalic acid that could not be detected with our GC-MS analysis method.

On the other hand, Figure 2a presents a Kinetic reaction of dimer 2 electrooxidation to determine conversion and product yield. As shown, after four hours most of the dimer ($\approx 90\%$ conversion) has reacted, with a high yield toward *p*-anisic acid ($\approx 84\%$). Furthermore, the figure shows the chronoamperometry of lignin dimer oxidation at 1.5V vs RHE. The electrochemical response is higher than the OER activity because of the reduction of onset potential. However, the current decreases as the dimer is consumed, reaching values similar to OER after two hours, when the conversion is approximately 80%.

Once β -O-4 linkages cleavage *via* dimeric models was studied, a model polymer (Pol G; entry 4, Table 1) formed solely by β -O-4 bonds connecting aromatic G structures (giving vanillin or vanillic acid as the only product) was synthesized to analyze the depolymerization and fragmentation of these linkages. This polymer was analyzed by gel permeation chromatography (GPC) and size exclusion chromatography (SEC) before and after 5 h of oxidation reaction (Figure 2b). The polymer chains are much smaller after the reaction (2-3 subunits mostly) compared to about 19 subunits it initially contained. Nevertheless, GC-MS results show a low monomers yield (≈ 5 -6%). As shown in Heteronuclear Single Quantum Coherence (2D-HSQC NMR) spectra⁴³ before and after the reaction (Figure S15), this polymer appears to contain different β - β' , α -O- γ' and γ -O- α' bonds produced during its complex synthesis that are not fragmented, thus avoiding significant production of monomers.

Table 1. Results of conversion and products yield about lignin models (dimers and polymer) and dioxasolv lignin electrooxidation.

Entry no.	Reactant	Time (h)	Conversion (%)		Yield (%)	
1		4	100		 (93)	-
2		4	100		 (84)	-
3		4	100		 (88)	-
4		5	Unreacted molecular weights	Initial molecular weights	Yield (%) mayortary products  3.2  2.1  5.1	
			$M_n \approx 411$	$M_n: 2551$		
			$M_w \approx 462$	$M_w: 3252$		
5	Lignin dioxasolv (Beech)	4	$M_w/M_n: 1.12$	$M_w/M_n: 1.27$		
			$M_n: 542$	$M_n: 1351$		
			$M_w: 651$	$M_w: 2785$		
6	Lignin dioxasolv (Pine)	4	$M_w/M_n: 1.20$	$M_w/M_n: 2.06$		
			$M_n: 376$	$M_n: 1140$		
			$M_w: 383$	$M_w: 2096$		

*Electrocatalyst: $\text{Ni}_{0.75}\text{Co}_{0.25}\text{OOH}/\text{CF}$. Electrolyte: 1M KOH. Sustrate: 0,01M lignin dimers (1,2,3), 2gL^{-1} Pol G, 2gL^{-1} lignin dioxasolv (5,6). H-cell with glass porous plate.

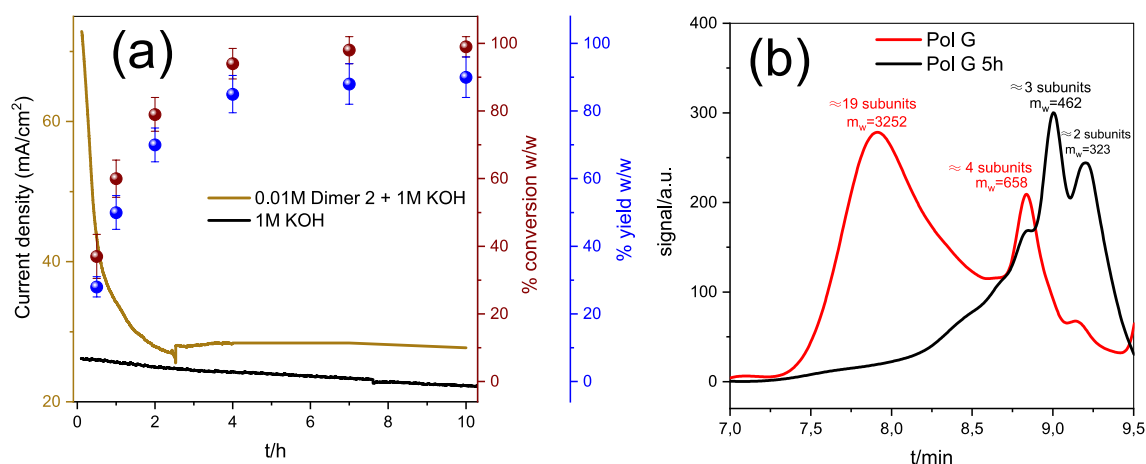


Figure 2. Dimer 2 and Pol G electrooxidation. (a) Kinetic reaction about dimer 2 electrooxidation, compared with OER. Conditions: 0,01M substrate, 1M KOH. (b) GPC analysis about Pol G before and after 5h of oxidation reaction. Conditions: 2g L^{-1} substrate, 1M KOH.

*Electrocatalyst: $\text{Ni}_{0.75}\text{Co}_{0.25}\text{OOH/CF}$.

Moreover, the adsorption behavior of dimer 2 over $\text{Ni}_{0.75}\text{Co}_{0.25}\text{OOH/CF}$ was studied by in-situ FTIR spectroscopy (Figure 3a) to obtain information about the possible reaction mechanism⁴⁴. As shown in Figure 3b, when a low potential is applied, besides the band corresponding to the skeletal vibration of the benzene ring (1504cm^{-1}), new ones appear towards to lower wavenumber ($1410\text{--}1471\text{cm}^{-1}$). These variations may be attributed to the interaction between Ni-Co and the benzene ring of the dimer that leads to the decrease of benzene symmetry, giving rise to band shifting and splitting⁴⁵. Furthermore, the $\nu(\text{C-O})$ band disappears or is shifted to a lower wavenumber, weakening the linkage⁴⁶. This observation suggests an interaction between the electrocatalyst surface and the oxygen linked to C_α ($\text{C}_\alpha\text{-O}$). For this reason, it seems that the dimer 2 is adsorbed by both the aromatic ring and $\text{C}_\alpha\text{-O}$. Experiments integrated with Spin-polarized density functional theory (DFT) studies should be carried out to study which of the two possible reaction mechanisms prevail.

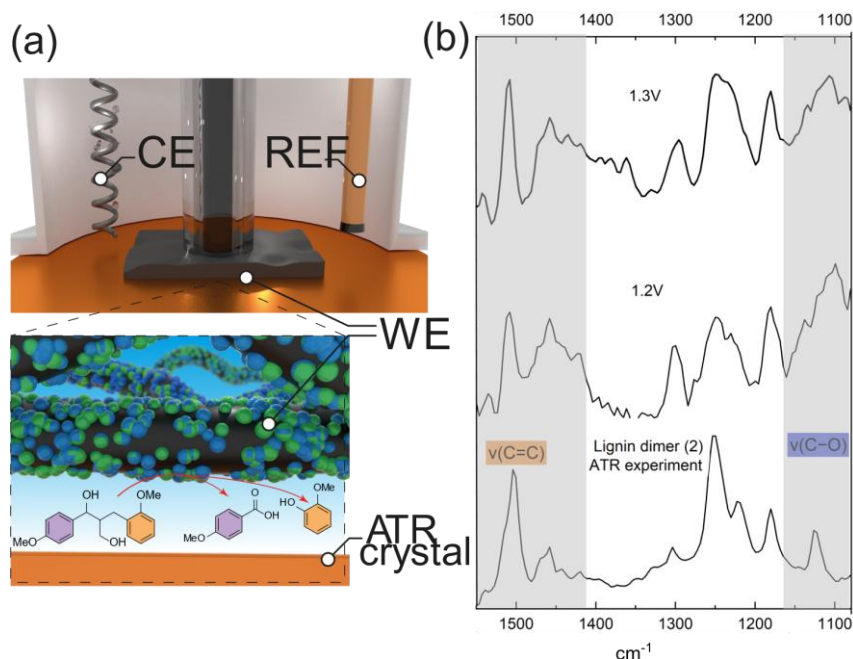


Figure 3. In-situ FTIR experiments. (a) In-situ FTIR configuration for dimer 2 electrooxidation. Cell: electrochemical glass purged with argon. Electrocatalyst: $\text{Ni}_{0.75}\text{Co}_{0.25}\text{OOH/CF}$. Three-electrode system: RHE and gold electrode as reference and counter electrodes, respectively. (b)

In-situ FTIR electrochemical experiments (chronoamperometry 5 min) compared with FTIR-ATR measure. Conditions: 0,01M dimer 2, 1M KOH.

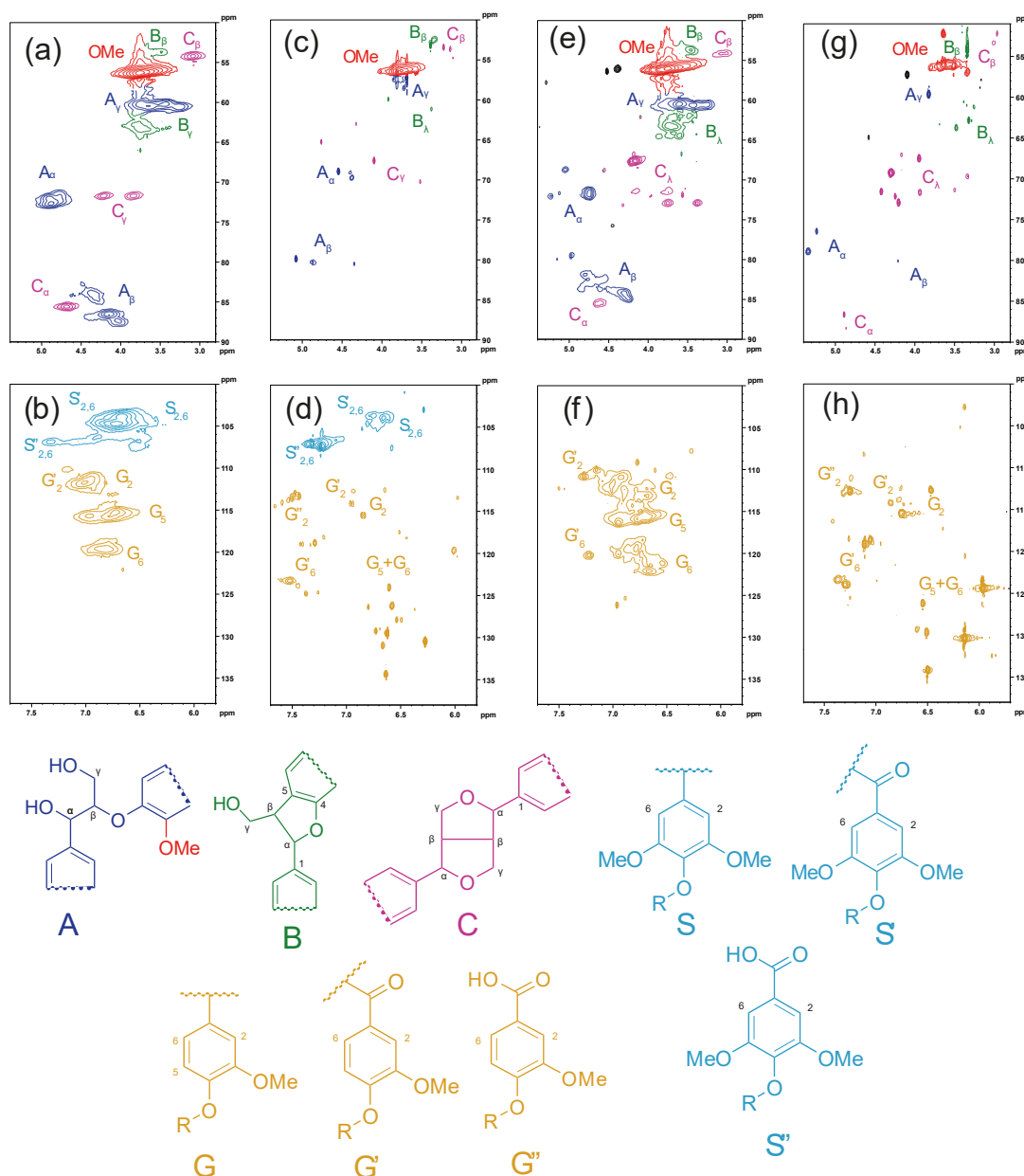


Figure 4. Main lignin substructures identified in the HSQC NMR spectra of the dioxasolv lignin: (A) β -O-4 linkages. (B) phenylcoumaran with α -O-4 and β -5 linkages. (C) resinol with β - β , α -O- γ , and γ -O- α linkages. (S) syringyl unit. (S') oxidized syringyl unit bearing a carboxylic group at C α . (S'') oxidized syringyl units bearing a carboxyl group at C α . (G) guaiacyl units. (G') oxidized guaiacyl unit bearing a carbonyl group at C α . (G'') oxidized guaiacyl unit bearing a carboxylic group at C α (a,b) beech lignin dioxasolv before reaction, (c,d) beech lignin dioxasolv after reaction, (e,f) pine lignin dioxasolv before reaction, (g,h) pine lignin dioxasolv after reaction. Conditions: 2g L⁻¹ lignin, 1M KOH.

Subsequently, the investigation focused on the depolymerization of lignin dioxasolv. Figure 4 displays the results of the HSQC before and after the reaction^{43,47,48}. This technique allows detecting signals that correspond to linkages in the lignin structure. The main interunit linkages observed in the beech and pine lignins are β -O-4, β -5, β - β , α -O- γ and γ -O- α structures. As can be seen in the aliphatic zone (Figure 4 a, c, e, and g), consequently to the depolymerization, about 70% of β -O-4 linkages have disappeared while β -5, β - β , α -O- γ , and γ -O- α linkages remain

(as in the case of Pol G). Furthermore, the aromatic zone (Figure 4 b, d, f, and h) manifests beech lignin presents both G and S aromatic units while pine lignin only contains G aromatic units because beech wood is hardwood and pine wood is softwood. It should be noted that after the reaction, there are a lot of signals of S2'' and G2'' due to most of the monomers obtained as electrooxidation results, containing a carboxylic group at C_α. In this line, monomeric degradation products were identified and quantified by GC-MS. As shown in Table 1, 4 h electrooxidation of beech dioxasolv led to a yield of vanillic acid and syringic acid of 2.1% w/w and 3.2% w/w, respectively, as majority products and 0.3 % w/w of vanillin and 0.5 % w/w of syringaldehyde as minority products which is equivalent to a yield of 70% compared to the total amount of monomers. Additionally, pine dioxasolv presents a yield of vanillic acid and vanillin of 5.1 % w/w and 0.5 % w/w, respectively (65% vs total amount of monomers). Moreover, precipitated lignin or unreacted lignin which were expected to have higher molecular weight and larger polarity compared to those in the organic phase, was also investigated (Table 1). As could be seen with the polymer, lignin chains are much smaller after the reaction (2-4 subunits for both beech and pine) compared to about 12-17 subunits it initially contained.

Last, depolymerization of lignin dioxasolv was studied by a Redox Flow system, which on an industrial scale would allow continuous work without stopping the reactor from isolating the products⁴⁹. Table 2 displays the results of the electrooxidation of lignin dioxasolv by chronopotentiometry in a Redox Flow system. In the case of beech lignin, extraction yields of 80% and 76% are achieved for vanillic and syringic acid, respectively, which are equivalent to 3.3 and 3.9% w/w concerning the initial weight of lignin. Similarly, when lignin pine is used, yields of 74% are achieved to produce vanillic acid, which is equivalent to 6.0% w/w rivaling in both with state-of-the-art but operating at room temperature^{26,27,50,51}.

Table 2. Results of the lignin electro-oxidation by chronopotentiometry in a Redox Flow system.

Lignin	Applied current (mA)	Time (h)	Yield of vanillic acid (VA) and vanillin (V) (%w/w ^a); Conversion (%)	Yield of syringic acid (SA) and syringaldehyde (S) (%w/w ^a); Conversion (%)
Beech Dioxanosolv	1000	5	V=0.4 ; VA=2.7 71%	S=0.7 ; SA=3.1 69%
Beech Dioxanosolv	250	20	V=0.2; VA=3.3 80%	S=0.3; SA=3.9 76%
Pine Dioxanosolv	1000	5	V=0.6; VA=5.1 67%	-
Pine Dioxanosolv	250	20	V=0.3; VA=6.0 74%	-

^a Referred to the initial weight of lignin (%w/w).

*Conversion: amount of VA + V or SA + S obtained with respect to that produced via the NBO method.

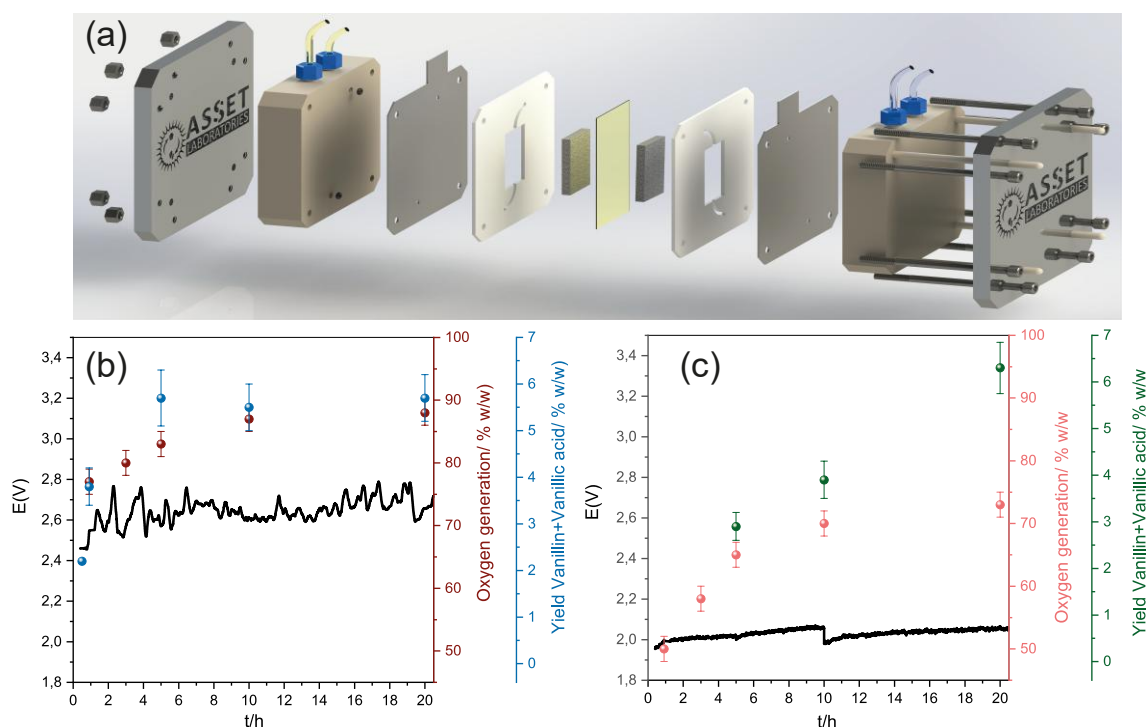


Figure 5. Lignin Pine dioxasolv electrooxidation by Redox Flow system. (a) Redox Flow system configuration. Two-electrode system: Working electrode: $Ni_{0.75}Co_{0.25}OOH/NF$ (6 cm^2); Counter electrode: $NiMo/NF$ (6 cm^2). Membrane: anion exchange membrane $50\text{ }\mu\text{m}$ thickness. Conditions: $10\text{--}40\text{ gL}^{-1}$ lignin, 1M KOH , 150 ml , 100 ml min^{-1} . (b) kinetic reaction to 1A. (c) kinetic reaction to 250mA.

Figure 5 shows different chronopotentiometry of pine dioxasolv (1A and 250mA) with voltage data, oxygen production, and the evolution of monomeric products. When 1A is applied (Figure 6a), higher yields are obtained in less time, producing around 5% w/w vanillic acid in 5 h. However, there is a lot of oxygen production hence, the faradic efficiency would be lower. The reason is that in a two-electrode system and working under chronopotentiometry there is no control over the oxidation potential to avoid the competition reaction (OER), as was possible with three-electrode system and chronoamperometry conditions. On the other hand, applying 250 mA, only 2.5% of vanillic acid is produced. Nevertheless, when the same coulombs have been used (20 h), vanillic acid production reaches 6% w/w. Efficiencies are higher at lower currents due to lower oxygen production and higher faradic efficiency. Moreover, the vanillin/vanillic acid ratio varies with reaction time because vanillin is inevitably oxidized to vanillic acid. For example, in 1 h to 1 A, there is 35% w/w vanillin compared to the total produced, and at 5 hours, approximately 10%.

Conclusions

In this study, a lignin electrooxidation method from a series of amorphous mixed-metal oxyhydroxides ($Fe_{1-x-y}Co_yNi_xOOH$) as electrocatalysts was developed. Initially, the optimization work carried out to evaluate the $C(OH)\text{--}C$ structure cleavage showed that Co, Ni oxyhydroxides are the most active electrocatalysts, manifesting $Ni_{0.75}Co_{0.25}OOH$, the best electrochemical performance and the highest product yields and faradaic efficiencies. In addition, it is possible to avoid the OER competition reaction because lignin models and organolv lignin oxidation present an earlier onset. In general, this method is capable of efficiently fragmenting the $\beta\text{--O--}4$ bonds of model lignin dimers and polymers (85%). Moreover, the experiments of lignin dioxasolv evidenced that 70% of $\beta\text{--O--}4$ linkages, approximately, have disappeared while $\beta\text{--}5$, $\beta\text{--}\beta$, $\alpha\text{--O--}\gamma$, and $\gamma\text{--O--}\alpha$ linkages remain. Therefore, it is a selective method for the fragmentation of $\beta\text{--O--}4$ bonds. Finally, for the Redox Flow system, monomer yields are 80% and 76% for vanillic and

syringic acid, respectively (3.3 and 3.9% w/w) for beech lignin and 74% to produce vanillic acid (6.0% w/w) for lignin pine, rivaling in both with state-of-the-art but operating at room temperature. Consequently, we can conclude the Ni-Co-Fe composition of the electrocatalyst has been successfully optimized to develop a method capable of selectively cleaving β -O-4 linkages and obtaining high monomeric yields working at room temperature without the use of noble metals and improving the results of Ni electrocatalysts.

Acknowledgements

N.G. thanks the support from grant “Ramon y Cajal” (RYC2018-023888-I) funded by MCIN/AEI/10.13039/501100011033. Likewise, N.G. wants to acknowledge the support received *via* the grants CNS2023-145354 and PID2021-128805NA-I00 funded by MCIN/AEI/10.13039/501100011033 and by the “European Union Next Generation EU/PRTR”. X.M. wants to acknowledge the support received *via* Spanish Ministerio de Ciencia e Innovación (PID2021-127332NB). This project has also received funding from the European Research Council (ERC) under the European Union’s Horizon 2020 research and innovation program (grant agreement No.948829).

Competing interests. The authors declare no competing interests.

Supplementary information The online version contains supplementary material.

Correspondence and requests for materials should be addressed to N.G.: nestor.guijarro@ua.es.

References

- (1) Qi, Y.; Guo, H.; Li, J.; Ma, L.; Xu, Y.; Liu, H.; Wang, C.; Zhang, Z. Recent Advances in the Electrocatalytic Oxidative Upgrading of Lignocellulosic Biomass. *ChemPhysMater* **2024**. <https://doi.org/10.1016/j.chphma.2024.02.001>.
- (2) Luo, J.; Liu, T. L. Electrochemical Valorization of Lignin: Status, Challenges, and Prospects. *Journal of Bioresources and Bioproducts* **2023**, *8* (1), 1–14. <https://doi.org/10.1016/j.jobab.2022.11.003>.
- (3) Xu, X.; Li, P.; Zhong, Y.; Yu, J.; Miao, C.; Tong, G. Review on the Oxidative Catalysis Methods of Converting Lignin into Vanillin. *Int J Biol Macromol* **2023**, *243*, 125203. <https://doi.org/10.1016/j.ijbiomac.2023.125203>.
- (4) Zhou, N.; Thilakarathna, W. P. D. W.; He, Q. S.; Rupasinghe, H. P. V. A Review: Depolymerization of Lignin to Generate High-Value Bio-Products: Opportunities, Challenges, and Prospects. *Front Energy Res* **2022**, *9*. <https://doi.org/10.3389/fenrg.2021.758744>.
- (5) Ragauskas, A. J.; Beckham, G. T.; Biddy, M. J.; Chandra, R.; Chen, F.; Davis, M. F.; Davison, B. H.; Dixon, R. A.; Gilna, P.; Keller, M.; Langan, P.; Naskar, A. K.; Saddler, J. N.; Tschaplinski, T. J.; Tuskan, G. A.; Wyman, C. E. Lignin Valorization: Improving Lignin Processing in the Biorefinery. *Science* (1979) **2014**, *344* (6185), 1246843. <https://doi.org/10.1126/science.1246843>.
- (6) Li, P.; Ren, J.; Jiang, Z.; Huang, L.; Wu, C.; Wu, W. Review on the Preparation of Fuels and Chemicals Based on Lignin. *RSC Adv* **2022**, *12* (17), 10289–10305. <https://doi.org/10.1039/D2RA01341J>.
- (7) Bajwa, D. S.; Pourhashem, G.; Ullah, A. H.; Bajwa, S. G. A Concise Review of Current Lignin Production, Applications, Products and Their Environmental Impact. *Ind Crops Prod* **2019**, *139*, 111526. <https://doi.org/10.1016/j.indcrop.2019.111526>.
- (8) *Petrochemiclas europe*. <https://www.petrochemistry.eu/we-build-the-future/>.

- (9) Ghahremani, R.; Staser, J. A. Electrochemical Oxidation of Lignin for the Production of Value-Added Chemicals on Ni-Co Bimetallic Electrocatalysts. **2018**, 72 (11), 951–960. <https://doi.org/doi:10.1515/hf-2018-0041>.
- (10) Zhu, H.; Wang, L.; Chen, Y.; Li, G.; Li, H.; Tang, Y.; Wan, P. Electrochemical Depolymerization of Lignin into Renewable Aromatic Compounds in a Non-Diaphragm Electrolytic Cell. *RSC Adv* **2014**, 4 (56), 29917–29924. <https://doi.org/10.1039/C4RA03793F>.
- (11) Garedew, M.; Lin, F.; Song, B.; DeWinter, T. M.; Jackson, J. E.; Saffron, C. M.; Lam, C. H.; Anastas, P. T. Greener Routes to Biomass Waste Valorization: Lignin Transformation Through Electrocatalysis for Renewable Chemicals and Fuels Production. *ChemSusChem* **2020**, 13 (17), 4214–4237. <https://doi.org/https://doi.org/10.1002/cssc.202000987>.
- (12) Li, C.; Zhao, X.; Wang, A.; Huber, G. W.; Zhang, T. Catalytic Transformation of Lignin for the Production of Chemicals and Fuels. *Chem Rev* **2015**, 115 (21), 11559–11624. <https://doi.org/10.1021/acs.chemrev.5b00155>.
- (13) Cao, Y.; Zhang, C.; Tsang, D. C. W.; Fan, J.; Clark, J. H.; Zhang, S. Hydrothermal Liquefaction of Lignin to Aromatic Chemicals: Impact of Lignin Structure. *Ind Eng Chem Res* **2020**, 59 (39), 16957–16969. <https://doi.org/10.1021/acs.iecr.0c01617>.
- (14) Li, T.; Takkellapati, S. The Current and Emerging Sources of Technical Lignins and Their Applications. *Biofuels, Bioproducts and Biorefining* **2018**, 12 (5), 756–787. <https://doi.org/https://doi.org/10.1002/bbb.1913>.
- (15) Garedew, M.; Lam, C. H.; Petitjean, L.; Huang, S.; Song, B.; Lin, F.; Jackson, J. E.; Saffron, C. M.; Anastas, P. T. Electrochemical Upgrading of Depolymerized Lignin: A Review of Model Compound Studies. *Green Chemistry* **2021**, 23 (8), 2868–2899. <https://doi.org/10.1039/D0GC04127K>.
- (16) Xu, R.; Zhang, K.; Liu, P.; Han, H.; Zhao, S.; Kakade, A.; Khan, A.; Du, D.; Li, X. Lignin Depolymerization and Utilization by Bacteria. *Bioresour Technol* **2018**, 269, 557–566. <https://doi.org/https://doi.org/10.1016/j.biortech.2018.08.118>.
- (17) Chen, Z.; Wan, C. Biological Valorization Strategies for Converting Lignin into Fuels and Chemicals. *Renewable and Sustainable Energy Reviews* **2017**, 73, 610–621. <https://doi.org/https://doi.org/10.1016/j.rser.2017.01.166>.
- (18) Gao, D.; Ouyang, D.; Zhao, X. Electro-Oxidative Depolymerization of Lignin for Production of Value-Added Chemicals. *Green Chemistry* **2022**, 24 (22), 8585–8605. <https://doi.org/10.1039/D2GC02660K>.
- (19) Tolba, R.; Tian, M.; Wen, J.; Jiang, Z.-H.; Chen, A. Electrochemical Oxidation of Lignin at IrO₂-Based Oxide Electrodes. *Journal of Electroanalytical Chemistry* **2010**, 649 (1), 9–15. <https://doi.org/https://doi.org/10.1016/j.jelechem.2009.12.013>.
- (20) Zhu, H.; Chen, Y.; Qin, T.; Wang, L.; Tang, Y.; Sun, Y.; Wan, P. Lignin Depolymerization via an Integrated Approach of Anode Oxidation and Electro-Generated H₂O₂ Oxidation. *RSC Adv* **2014**, 4 (12), 6232–6238. <https://doi.org/10.1039/C3RA47516F>.
- (21) Liu, M.; Wen, Y.; Qi, J.; Zhang, S.; Li, G. Fine Chemicals Prepared by Bamboo Lignin Degradation through Electrocatalytic Redox between Cu Cathode and Pb/PbO₂ Anode in Alkali Solution. *ChemistrySelect* **2017**, 2 (17), 4956–4962. <https://doi.org/https://doi.org/10.1002/slct.201700881>.
- (22) Cai, P.; Fan, H.; Cao, S.; Qi, J.; Zhang, S.; Li, G. Electrochemical Conversion of Corn Stover Lignin to Biomass-Based Chemicals between Cu/NiMoCo Cathode and Pb/PbO₂ Anode in Alkali Solution. *Electrochim Acta* **2018**, 264, 128–139. <https://doi.org/https://doi.org/10.1016/j.electacta.2018.01.111>.
- (23) Jia, Y.; Wen, Y.; Han, X.; Qi, J.; Liu, Z.; Zhang, S.; Li, G. Electrocatalytic Degradation of Rice Straw Lignin in Alkaline Solution through Oxidation on a Ti/SnO₂–Sb₂O₃/α-PbO₂/β-PbO₂ Anode and Reduction on an Iron or Tin Doped Titanium Cathode. *Catal Sci Technol* **2018**, 8 (18), 4665–4677. <https://doi.org/10.1039/C8CY00307F>.
- (24) Lan, C.; Fan, H.; Shang, Y.; Shen, D.; Li, G. Electrochemically Catalyzed Conversion of Cornstalk Lignin to Aromatic Compounds: An Integrated Process of Anodic Oxidation of a

- Pb/PbO₂ Electrode and Hydrogenation of a Nickel Cathode in Sodium Hydroxide Solution. *Sustain Energy Fuels* **2020**, 4 (4), 1828–1836. <https://doi.org/10.1039/C9SE00942F>.
- (25) Zirbes, M.; Schmitt, D.; Beiser, N.; Pitton, D.; Hoffmann, T.; Waldvogel, S. R. Anodic Degradation of Lignin at Active Transition Metal-Based Alloys and Performance-Enhanced Anodes. *ChemElectroChem* **2019**, 6 (1), 155–161. <https://doi.org/https://doi.org/10.1002/celec.201801218>.
- (26) Smith, C. Z.; Utley, J. H. P.; Hammond, J. K. Electro-Organic Reactions. Part 60[1]. The Electro-Oxidative Conversion at Laboratory Scale of a Lignosulfonate into Vanillin in an FM01 Filter Press Flow Reactor: Preparative and Mechanistic Aspects. *J Appl Electrochem* **2011**, 41 (4), 363–375. <https://doi.org/10.1007/s10800-010-0245-0>.
- (27) Zirbes, M.; Quadri, L. L.; Breiner, M.; Stenglein, A.; Bomm, A.; Schade, W.; Waldvogel, S. R. High-Temperature Electrolysis of Kraft Lignin for Selective Vanillin Formation. *ACS Sustain Chem Eng* **2020**, 8 (19), 7300–7307. <https://doi.org/10.1021/acssuschemeng.0c00162>.
- (28) Zhang, J.; Suo, C.; Sun, J.; Li, W.; Luo, S.; Ma, C.; Liu, S. Electrocatalysis C α –C β and C β –O Bond Cleavage of Lignin Model Compound Using Ni-Co/C as Catalyst Electrode in Deep Eutectic Solventx. *Journal of Electroanalytical Chemistry* **2023**, 938, 117385. <https://doi.org/https://doi.org/10.1016/j.jelechem.2023.117385>.
- (29) Honorato, A. M.; Khalid, M.; Curvelo, A. A.; Varela, H.; Shahgaldi, S. Trimetallic Nanoalloy of NiFeCo Embedded in Phosphidated Nitrogen Doped Carbon Catalyst for Efficient Electro-Oxidation of Kraft Lignin. *Polymers*. **2022**. <https://doi.org/10.3390/polym14183781>.
- (30) Breiner, M.; Zirbes, M.; Waldvogel, S. R. Comprehensive Valorisation of Technically Relevant Organosolv Lignins via Anodic Oxidation. *Green Chemistry* **2021**, 23 (17), 6449–6455. <https://doi.org/10.1039/D1GC01995C>.
- (31) Ghahremani, R.; Staser, J. A. Electrochemical Oxidation of Lignin for the Production of Value-Added Chemicals on Ni-Co Bimetallic Electrocatalysts. **2018**, 72 (11), 951–960. <https://doi.org/doi:10.1515/hf-2018-0041>.
- (32) Di Fidio, N.; Timmermans, J. W.; Antonetti, C.; Raspolli Galletti, A. M.; Gosselink, R. J. A.; Bisselink, R. J. M.; Slaghek, T. M. Electro-Oxidative Depolymerisation of Technical Lignin in Water Using Platinum, Nickel Oxide Hydroxide and Graphite Electrodes. *New Journal of Chemistry* **2021**, 45 (21), 9647–9657. <https://doi.org/10.1039/D1NJ01037A>.
- (33) Smith, R. D. L.; Prévot, M. S.; Fagan, R. D.; Zhang, Z.; Sedach, P. A.; Siu, M. K. J.; Trudel, S.; Berlinguette, C. P. Photochemical Route for Accessing Amorphous Metal Oxide Materials for Water Oxidation Catalysis. *Science (1979)* **2013**, 340 (6128), 60–63. <https://doi.org/10.1126/science.1233638>.
- (34) Zhang, X.; Zhong, H.; Zhang, Q.; Zhang, Q.; Wu, C.; Yu, J.; Ma, Y.; An, H.; Wang, H.; Zou, Y.; Diao, C.; Chen, J.; Yu, Z. G.; Xi, S.; Wang, X.; Xue, J. High-Spin Co³⁺ in Cobalt Oxyhydroxide for Efficient Water Oxidation. *Nat Commun* **2024**, 15 (1), 1383. <https://doi.org/10.1038/s41467-024-45702-4>.
- (35) Trafela, Š.; Zavašnik, J.; Šturm, S.; Rožman, K. Ž. Formation of a Ni(OH)₂/NiOOH Active Redox Couple on Nickel Nanowires for Formaldehyde Detection in Alkaline Media. *Electrochim Acta* **2019**, 309, 346–353. <https://doi.org/https://doi.org/10.1016/j.electacta.2019.04.060>.
- (36) Chung, Y.-H.; Jang, I.; Jang, J.-H.; Park, H. S.; Ham, H. C.; Jang, J. H.; Lee, Y.-K.; Yoo, S. J. Anomalous in Situ Activation of Carbon-Supported Ni₂P Nanoparticles for Oxygen Evolving Electrocatalysis in Alkaline Media. *Sci Rep* **2017**, 7 (1), 8236. <https://doi.org/10.1038/s41598-017-08296-0>.
- (37) Zhou, H.; Li, Z.; Xu, S. M.; Lu, L.; Xu, M.; Ji, K.; Ge, R.; Yan, Y.; Ma, L.; Kong, X.; Zheng, L.; Duan, H. Selectively Upgrading Lignin Derivatives to Carboxylates through Electrochemical Oxidative C(OH)–C Bond Cleavage by a Mn-Doped Cobalt Oxyhydroxide

- Catalyst. *Angewandte Chemie - International Edition* **2021**, 60 (16), 8976–8982. <https://doi.org/10.1002/anie.202015431>.
- (38) Smith, R. D. L.; Prévot, M. S.; Fagan, R. D.; Trudel, S.; Berlinguette, C. P. Water Oxidation Catalysis: Electrocatalytic Response to Metal Stoichiometry in Amorphous Metal Oxide Films Containing Iron, Cobalt, and Nickel. *J Am Chem Soc* **2013**, 135 (31), 11580–11586. <https://doi.org/10.1021/ja403102j>.
 - (39) Gazi, S.; Hung Ng, W. K.; Ganguly, R.; Putra Moeljadi, A. M.; Hirao, H.; Soo, H. Sen. Selective Photocatalytic C–C Bond Cleavage under Ambient Conditions with Earth Abundant Vanadium Complexes. *Chem Sci* **2015**, 6 (12), 7130–7142. <https://doi.org/10.1039/C5SC02923F>.
 - (40) Danlu, Z.; Xu, Z.; Sinong, W.; Yan, X.; Qiqi, D.; Fengxia, Y.; Peng, W.; Chuanfu, L.; Wu, L. Electrochemical Oxidation of Lignin Model Compounds over Metal Oxyhydroxides on Nickel Foam. *Green Chemistry* **2024**, 26 (13), 7759–7768. <https://doi.org/10.1039/D4GC02156H>.
 - (41) Chen, K.; Cao, M.; Ding, C.; Zheng, X. A Green Approach for the Synthesis of Novel Ag₃PO₄/SnO₂/Porcine Bone and Its Exploitation as a Catalyst in the Photodegradation of Lignosulfonate into Alkyl Acids. *RSC Adv* **2018**, 8 (47), 26782–26792. <https://doi.org/10.1039/C8RA04962A>.
 - (42) Su, J.; Yang, L.; Liu, R. N.; Lin, H. Low-Temperature Oxidation of Guaiacol to Maleic Acid over TS-1 Catalyst in Alkaline Aqueous H₂O₂ Solutions. *Chinese Journal of Catalysis* **2014**, 35 (5), 622–630. [https://doi.org/https://doi.org/10.1016/S1872-2067\(14\)60039-5](https://doi.org/https://doi.org/10.1016/S1872-2067(14)60039-5).
 - (43) Yuan, T.-Q.; Sun, S.-N.; Xu, F.; Sun, R.-C. Characterization of Lignin Structures and Lignin–Carbohydrate Complex (LCC) Linkages by Quantitative ¹³C and 2D HSQC NMR Spectroscopy. *J Agric Food Chem* **2011**, 59 (19), 10604–10614. <https://doi.org/10.1021/jf2031549>.
 - (44) Peng, T.; Zhang, W.; Liang, B.; Lian, G.; Zhang, Y.; Zhao, W. Electrocatalytic Valorization of Lignocellulose-Derived Aromatics at Industrial-Scale Current Densities. *Nat Commun* **2023**, 14 (1), 7229. <https://doi.org/10.1038/s41467-023-43136-y>.
 - (45) Li, Z.; Yan, Y.; Xu, S.-M.; Zhou, H.; Xu, M.; Ma, L.; Shao, M.; Kong, X.; Wang, B.; Zheng, L.; Duan, H. Alcohols Electrooxidation Coupled with H₂ Production at High Current Densities Promoted by a Cooperative Catalyst. *Nat Commun* **2022**, 13 (1), 147. <https://doi.org/10.1038/s41467-021-27806-3>.
 - (46) Li, H.; Qin, F.; Yang, Z.; Cui, X.; Wang, J.; Zhang, L. New Reaction Pathway Induced by Plasmon for Selective Benzyl Alcohol Oxidation on BiOCl Possessing Oxygen Vacancies. *J Am Chem Soc* **2017**, 139 (9), 3513–3521. <https://doi.org/10.1021/jacs.6b12850>.
 - (47) Zhao, W.; Xiao, L.-P.; Song, G.; Sun, R.-C.; He, L.; Singh, S.; Simmons, B. A.; Cheng, G. From Lignin Subunits to Aggregates: Insights into Lignin Solubilization. *Green Chemistry* **2017**, 19 (14), 3272–3281. <https://doi.org/10.1039/C7GC00944E>.
 - (48) Talebi Amiri, M.; Bertella, S.; Questell-Santiago, Y. M.; Luterbacher, J. S. Establishing Lignin Structure-Upgradeability Relationships Using Quantitative ¹H–¹³C Heteronuclear Single Quantum Coherence Nuclear Magnetic Resonance (HSQC-NMR) Spectroscopy. *Chem Sci* **2019**, 10 (35), 8135–8142. <https://doi.org/10.1039/C9SC02088H>.
 - (49) Wang, D.; Wang, P.; Wang, S.; Chen, Y.-H.; Zhang, H.; Lei, A. Direct Electrochemical Oxidation of Alcohols with Hydrogen Evolution in Continuous-Flow Reactor. *Nat Commun* **2019**, 10 (1), 2796. <https://doi.org/10.1038/s41467-019-10928-0>.
 - (50) Beliaeva, K.; Grimaldos-Orsorio, N.; Ruiz-López, E.; Burel, L.; Vernoux, P.; Caravaca, A. New Insights into Lignin Electrolysis on Nickel-Based Electrocatalysts: Electrochemical Performances before and after Oxygen Evolution. *Int J Hydrogen Energy* **2021**, 46 (72), 35752–35764. <https://doi.org/https://doi.org/10.1016/j.ijhydene.2021.01.224>.
 - (51) Gunerhan, A.; Altuntas, O.; Açıkkalp, E. A Comprehensive Analysis of the Production of H₂ and Value-Added Chemicals from the Electrolysis of Biomass and Derived Feedstocks.

Biomass Bioenergy **2025**, 192, 107510.
<https://doi.org/https://doi.org/10.1016/j.biombioe.2024.107510>.